UNDERSTANDING GLACIER SLIDING FROM SUBGLACIALLY DEPOSITED SILT SKINS

CARISSA CARTER
Department of Geosciences, Wiliams College
Faculty Sponsor: David Dethier, Williams College

INTRODUCTION

Glacial advances and retreats, prominent factors in global climate and sea level change, are controlled by climate and a combination of processes including ice deformation, basal sliding, and subglacial hydraulic systems. Evidence of the effects of these processes is preserved in the landforms and deposits left behind. Examining deposits recently uncovered by retreating glaciers is one method of studying subglacial processes and glacier sliding. Features of subglacial deposits, including their distribution, morphology, and chemistry, provide specific clues about the interaction of ice, the bedrock it flows over, and subglacial water. Morphology of subglacial deposits is a key to understanding the larger aspects of glacier systems, and how they, in turn, have affected global climate throughout Earth history (Paterson, 1994).

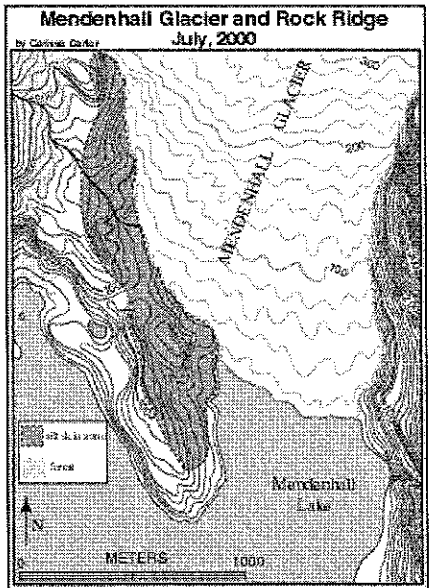

Fig. 1 ROCK RIDGE DEPICTING SILTSKIN ZONES
Map depicting zones where silt skins are found on the Mendenhall rock ridge. Ice was at western extent of silt skin zone approximately 20 years ago.

Location and Sample Description

In the past two decades, the retreating Mendenhall Glacier in Juneau, Alaska has exposed a bedrock ridge spotted with patchy coatings of calcite-cemented clay to sand-sized lithic grains (Fig. 1). These coatings, referred to here as 'silt skins', range from 0.5 to 20 mm in thickness and display two distinct morphologies: striated and corrugated. Striated silt skins are thin, located mainly on stoss slopes, and preserve local striation direction. Thicker, corrugated skins form on lee slopes and consist of parallel micro-ridges elongated in the local downslope direction (Fig. 2a). Micro-ridges are constructional features enhanced by erosional processes; wavelengths generally range from 1 to 10 mm.

METHODS

Field Work

I collected silt skin data by mapping their distribution on the bedrock ridge, recording Global Positioning System (GPS) locations, and collecting skin, rock, ice, and water samples. I made transects at regular intervals over the entire rock ridge normal to the ice front. Transects consisted of 8 to 12 measurement points; at each point I collected a GPS location, measured local slope, and local striation direction. Additionally, I estimated a percentage cover value for silt skins by placing a one-meter square frame on the rock face exposing a local maximum cover, and then making an estimate using a 'Comparison Chart for Estimating Percentage Composition'. At collection localities, I noted orientation-, striation-, and local downslope-direction on individual samples.

I also used a GPS receiver to map the ice front, denote the extent of an area of high skin density, and determine the 'zero skin line' where coatings are no longer preserved.

Additionally, I gathered three ice samples, including a basal sample from the ice front on the western side of the glacier, a basal sample from the ice front at approximately mid-glacier, and one mid-ice sample from the ice front at mid-glacier. I traversed to the West Side of the glacier and collected a subglacial water sample by crawling under the ice.

Figure 2. Tree ring width vs. retreat rate

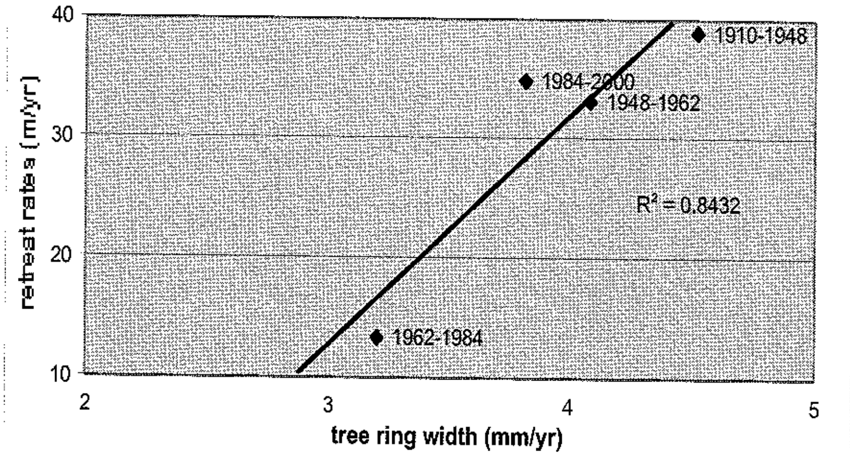

REFERENCES CITED

Anderson, B.G., and Borns, Jr., H.W., 1994, The ice age world: Oslo, Scandinavian University Press, 208 p.

Bennett, M.R., and Glasser, N.F., 1996, Glacial geology: Ice sheets and landforms: Chichester, John Wiley & Sons, 365 p.

Knopf, Adolph, 1912, The Eagle River region, southeastern Alaska: United States Geological Survey Bulletin 502, 61 p.

Lawrence, D.B., 1950, Glacier fluctuation for six centuries in southeastern Alaska and its relation to solar activity: The Geographical Review, v. 40, no. 2, p. 191-223.

Miller, R.D., 1975, Surficial geologic map of the Juneau urban area and vicinity, Alaska: United States Geologic Survey Miscellaneous Investigation Series Map 1-885.

Wiles, G.C., Calkin, P.E., and Jacoby, G.C., 1996, Tree-ring analysis and Quaternary geology: Principles and recent applications: Geomorphology, v. 16, p. 259-272.

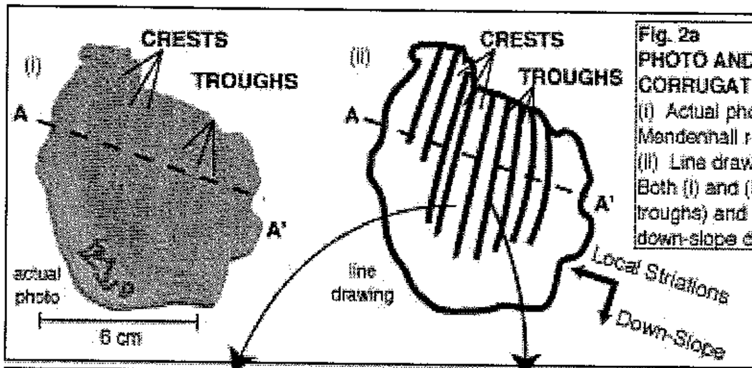

Fig. 2a
PHOTO AND LINE DRAWING DEPICTING CORRUGATED SILT SKIN FEATURES
(i) Actual photo of corrugated silt skin taken oriented from Mendenhall rock ridge
(ii) Line drawing of corrugated silt skin
Both (i) and (ii) depict parallel microridges (crests and troughs) and indicate local striation direction and local down-slope direction.

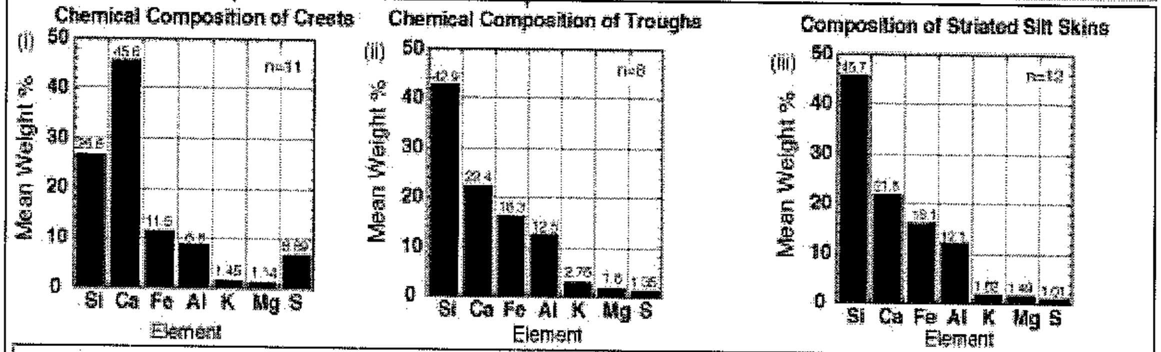

Fig. 2b. CHEMICAL COMPOSITION OF CRESTS, TROUGHS, AND STRIATED SILT SKINS
(i) Crests have a Ca/Si ratio of 1.71 : 1 and a noticeable S peak which may indicate the presence of organic matter. (ii) Troughs have a Ca/Si ratio of 0.52 : 1, and (iii) Striated silt skins have a similar composition to troughs.

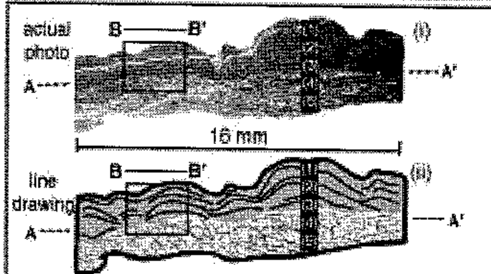

Ca/Si Ratio	
(1)	2.86 / 1
(2)	1.25 / 1
(3)	1.24 / 1
(4)	4.60 / 1
(5)	2.09 / 1

Fig. 2c. SILT SKIN THIN SECTION DEPICTING CA/SI RATIOS AND INTERNAL STRUCTURE
In (i) actual photo of thin section and (ii) line drawing highlighting prominant features, note the presence of a bottom, calcite-rich, massive layer, and a top, laminated layer less dominant in calcite. This transect also shows a Ca spike at the top of a crest. In both, A-A' corresponds to sample shown in Fig. 2a.

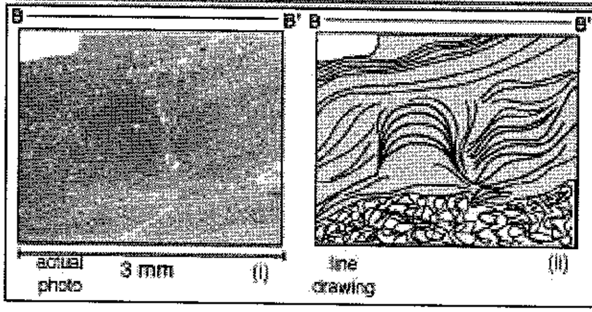

Fig. 2d. SILT SKIN THIN SECTION HIGHLIGHTING MICROLAMINATIONS AND COMPLEX INTERNAL STRUCTURE
(i) Actual photo of thin section and (ii) line drawing highlighting laminations and prominant features show internal structure of silt skin. Prominant hump resembles organic bacterial mats but may be a feature of soft sediment deformation or a product of subglacial cross-bedding in the regelation layer. Layers alternate dark and light in color suggesting either a cyclical change in grain size or organic layers interbedded with silt and clay.

Laboratory Work

I mounted and coated selected samples with Au-Pd for analysis with the Cambridge Stereoscan 100 Scanning Electron Microscope (SEM) and the Princeton Gamma Tech Avalon Energy Dispersive Spectrometer (EDS) using a Tracor SiLi crystal detector with a berylium window. I made images, dot maps, and ran semi-quantitative analyses at regular transect intervals on corrugated, striated, and cross-sectional portions of silt skins as well as on sediment filtered from water and ice samples, and processed all data with PGT Excalibur and Avalon software. For each EDS analysis I sampled an area approximately 80_ m^2 at 1.10kx-1.20kx magnification with a tilt angle of 10-12° and dead time of 30-40%.

I conducted grain size analyses by point counting, and examined silt skin structure on thin sections prepared by Spectrum Petrographics. I calculated grain size distribution using a sampling of 700 randomly selected grains.

I filtered melted ice and water samples using a 0.45 _ m filter and weighed each filter paper on a top-loading balance. I allowed each of the four melted and filtered samples to reach room temperature, measured out 50 ml of each, and determined pH using an air-equilibriated instrument in the lab. I calculated the acid neutralizing capacity (ANC) by titrating each sample to pH 4.5 with sulfuric acid, and then solved for $CaCO_3$ content. Using another 100 ml of each sample, I filtered the water a second time with 0.45 _ m glass microfiber filters and analyzed the resultant water samples for cations by atomic absorption using a Perkin Elmer AAnalyst 300 and anions with a Dionex IC 550 ion chromatograph.

Utilizing Pathfinder Office, Arcview GIS, and Adobe Illustrator, I processed my GPS measurements and related data, and created an up-to-date map of the Mendenhall rock ridge area and ice front as of July, 2000 (Fig. 1). This map will be used to model former ice positions and to model the extent of subglacial cavity systems on the Mendenhall rock ridge.

Finally, I selected silt skin samples for C and O isotope analysis. I prepared ten grams of five samples by scraping off organic matter on the silt skin surface, and then crushing with a mortar and pestle.

RESULTS

Silt Skin Composition and Structure

From EDS analysis it is clear that the surface composition of silt skin crests and troughs differs mainly with respect to the Ca/Si ratio (Fig. 2b). Crests have a Ca/Si ratio of 1.7 in terms of mean weight percent, while troughs have a ratio of 0.52/1. Striated silt skins reveal surface compositions much like trough composition. These numbers in conjunction with Al values (8.8% in crests and 12.5% in troughs), suggest that crests are either concentrating or preserving calcite cement, while troughs have a higher fraction of mud and clay. While Fe, K, and Mg are fairly consistent in both crests and troughs, S values in crests are noticeably higher than in troughs (6.69% vs. 1.35%). This might suggest the presence of organic matter, possibly bacterial mats, in silt skin samples, or it may simply signify the presence of pyrite.

Thin sections show that silt skins possess a series of microlaminae and complex internal structures, as well as displaying chemical compositional differences from the bottom (rock contact) portion of the skin to the top (Fig. 2c). Skins are composed of two larger zones: the bottom, a calcite-rich, lighter, massive zone; and the top, a less calcite-rich, darker, laminated zone. The layers in the top zone alternate dark and light in color, and thicknesses range from 2_ m to 2mm. These layers may represent differences in grain size, or they might indicate the presence of organic matter interbedded with silt and clay grains. Transects taken across cross-sectional areas of silt skins using EDS confirm the presence of a calcite-rich bottom layer, and also reflect calcite concentration at the surface of crests.

The structures present in the layered portion of silt skins are non-uniform. Some areas are simply cross-bedded, others display soft-sediment deformation structures, and still others resemble, on a microscale, features found in stromatolite mats (Fig. 2d).

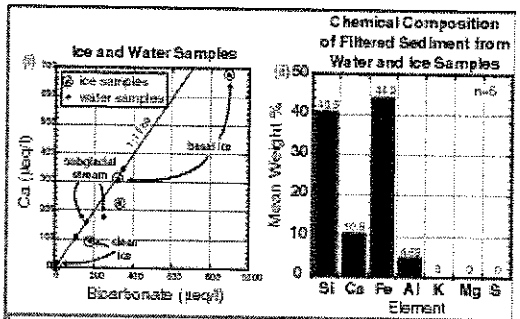

Fig. 3 CHEMICAL ANALYSIS OF ICE AND WATER SAMPLES, AND FILTERED SEDIMENT COMPOSITION
(i) Plot of Ca and Bicarbonate for water and ice samples. Charge balances range from -9% to -23%. (Some samples collected and titrated by Seth Atkinson).
(ii) Filtered sediment is high in Fe and has a Ca/Si ratio of 0.26 : 1.

Ice and Water Samples

Chemical analysis of the filtered ice and water samples reveals that samples lie on the 1:1 correlation line between Ca (_ eq/l) and HCO_3^- (_ eq/l) (Fig. 3). This indicates that they all originated in the same system. Charge balances in each of the samples ranges from –9% to –23%. Although low in concentration in the garnet-staurolite grade meta-sediments of the area, the calcium present in ice and water samples, and the calcite cement in silt skins may originate in the bedrock (Brown, Sharp and Tranter, 1996).

EDS analysis of sediment filtered from the ice and water samples reveals a Si/Ca ratio of 0.26/1 (Fig. 3).

SILT SKIN FORMATION

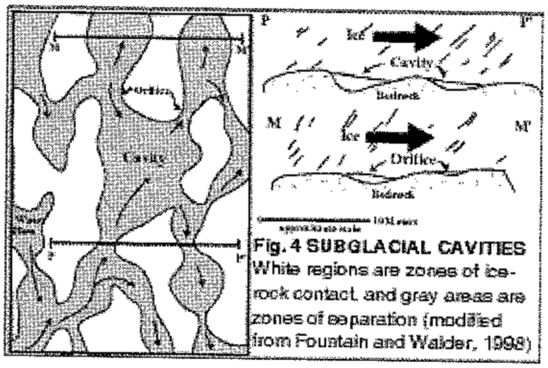

Fig. 4 SUBGLACIAL CAVITIES
White regions are zones of ice-rock contact, and gray areas are zones of separation (modified from Fountain and Walder, 1998)

Silt skins at the Mendenhall Glacier developed in the former subglacial cavity system from processes likely related to regelation flow and cyclical fluctuations in subglacial water pressure. The bedrock ridge where I mapped silt skins is not smooth, and cavity systems were probably widespread when the glacier covered the area. Cavities open when moving ice separates from the glacier bed, and close when the ice creeps into the cavity (Fig. 4). Consequently, very rough beds and fast moving glaciers are conducive to cavity formation (Fountain and Walder, 1998). If I can model the extent of paleo-cavities on the Mendenhall rock ridge, and estimate the temporal and annual changes in the amount of subglacial water flow, then I will be able to identify the subglacial processes that were active when the glacier covered the ridge, and classify the conditions under which silt skins form.

In regelation, ice on stoss slopes of small bedrock bumps (_ 1 meter) is forced by the slightly increased pressure to melt. The thin water film flows around to the lee slope of the obstacle, where decreased pressure allows it to refreeze (Paterson, 1994).

Carbonate coatings morphologically similar to silt skins have been described by Hallet (1976) at temperate glaciers in Alberta and the northern United States, and attributed to subglacial precipitation of $CaCO_3$ on limestone bedrock, pressure melting, and regelation. Lee-slope freezing of the regelation layer has a strong effect on the chemical composition of the meltwater and its degree of saturation because of the concentration of impurities and solutes during freezing. Specifically, freezing concentrates solutes in the liquid phase until they are concentrated enough to precipitate from solution. Hallet (1976) performed experiments where dilute $CaCO_3$ solutions were slowly frozen. He found that as ice accumulates and freezing progresses, the Ca^{++} ion concentration can increase up to 50 times that of the original solution. Basically, continuous freezing and rejection of solutes from the ice greatly enriches the meltwater in solutes, and the precipitates then formed could have a role in reducing the sliding velocity of the glacier (Hallet, 1976).

The absence limestone in the nearby substrate in conjunction with the mineral composition of the skins and their unique corrugation structure suggests that processes in the cavity system of the Mendenhall Glacier are related to but different from those explained in the study of Hallet (1976).

Silt skin formation in my study area is related to regelation processes and the development of cavities in subglacial hydraulic systems. However, the source of the calcite cement, development of corrugation structures, and their relationship to subglacial processes is not fully understood. My project explores these features and processes at the Mendenhall Glacier and their relationship to the processes of subglacial sliding and water flow. Therefore, while they do not persist in subaerial exposures for longer than ~ 20 years near the Mendenhall Glacier, silt skins may provide a useful tool for understanding the dynamics of glacier flow over bedrock.

REFERENCES CITED

Brown, G. H., Sharp, M., and Tranter, M., 1996, Subglacial chemical erosion: seasonal variations in solute provenance, Haut Glacier d'Arolla, Valais, Switzerland: Annals of Glaciology, v. 22, p. 25-31.

Fountain, A. G., and Walder, J. S., 1998, Water flow through temperate glaciers: Reviews of Geophysics, v. 36, no. 3, p. 299-328.

Hallet, B., 1976, The effect of subglacial chemical processes on glacier sliding.: Journal of Glaciology, v. 17, p. 209-221.

Paterson, W. S. B., 1994, The Physics of Glaciers: Tarrytown, Pergamon/Elsevier Science Ltd., 472 p.